Research Article

Naser F. Al-Tannak*, John V. Anyam, Eman Y. Santali, Alexander I. Gray, Collins U. Ibeji, John O. Igoli

Anti-parasitic activity and computational studies on a novel labdane diterpene from the roots of *Vachellia nilotica*

https://doi.org/10.1515/chem-2024-0005
received October 17, 2023; accepted March 8, 2024

Abstract: A new labdane diterpene characterized as 18α-*O*-*trans*-*p*-feruloyl-15-methyl-8(17)-labdanoate has been isolated from the roots of *Vachellia nilotica*. Also isolated were *p*-coumaric acid, ferulic acid, stearic acid, lupeol, and a mixture of β-sitosterol and stigmasterol. The compounds were obtained after a series of column chromatography on silica gel, and their structures were elucidated using NMR and LC-MS analyses. The new diterpene showed good anti-parasitic activity with an IC_{50} of 0.0177 µM against *Trypanosoma brucei* and 0.0154 µM against *Leishmania major* using an Alamar Blue assay. The compound also displayed very good inhibitory activity against *Leishmania major* compared to *Trypanosoma brucei rhodesiense* with a binding energy of −10.5 and −7.8 kcal/mol, respectively. Density functional theory analysis showed that the studied compound has low LUMO–HOMO energy, signifying a high chemical reactivity with the ability to donate electrons to electron-accepting species.

Keywords: labdane diterpenes, phenylpropanoids, ferulic acid, anti-parasitic activity, *Vachellia nilotica*

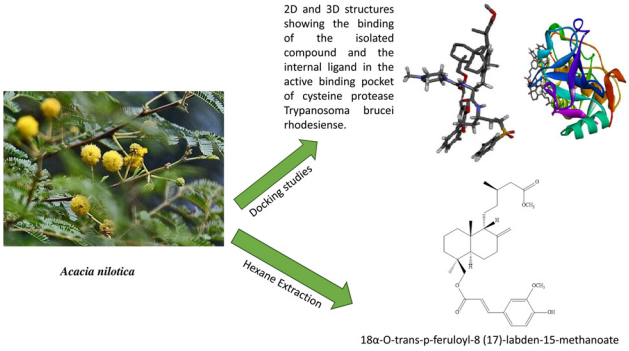

Graphical abstract

1 Introduction

Ethnopharmacological practices have been a basis for drugs, and there is presently a rekindled interest in drug discovery from natural products [1,2]. A present drug discovery strategy is the *in silico* or computer-aided drug design (CADD) screening of compounds or libraries for active moieties and identifying pharmacophores pertinent for drug action [3,4] or any toxic properties [5,6]. Natural product libraries or boxes are also being created and interrogated for compounds with diverse chemical space and activities that they could provide. Thus, the isolation of novel natural compounds to add to the growing natural compound libraries and introduce more chemical space or diversity via CADD and *in vitro* screening is a new approach to drug discovery from natural compounds. *Vachellia nilotica* (L.) P.J.H.Hurter & Mabb. (Syn: *Acacia nilotica* Linn.) (Fabaceae), commonly known as Egyptian mimosa or thorn, grows freely in Nigeria, Egypt, and South Africa. It is also found or introduced in several other countries, regions, and continents [7]. The plant is a small to medium tree, 7–13 m tall, with a girth of 20–30 cm [8]. The plant attracts ants and other pests [9]. There are several ethnobotanical reports on the plant, including treatment of abdominal pains, diarrhoea, dysentery, genital and urinary tract infections, and as an expectorant [10]. In a previous

* **Corresponding author: Naser F. Al-Tannak,** Department of Pharmaceutical Chemistry, Faculty of Pharmacy, Health Science Center, Kuwait University, Jabriya, Kuwait, e-mail: Dr.altannak@ku.edu.kw
John V. Anyam, John O. Igoli: Department of Chemistry, Joseph Sarwuan Tarka University Makurdi, PMB 2373, Benue State, Nigeria
Eman Y. Santali: Department of Pharmaceutical Chemistry, College of Pharmacy, Taif University, P.O. Box 11099, Taif 21944, Saudi Arabia
Alexander I. Gray: Strathclyde Institute of Pharmacy and Biomedical Sciences, University of Strathclyde, Glasgow, United Kingdom
Collins U. Ibeji: Department of Pure and Industrial Chemistry, Faculty of Physical Sciences, University of Nigeria, Nsukka 410001, Enugu State, Nigeria; Catalysis and Peptide Research Unit, School of Health Sciences, University of KwaZulu-Natal, Westville Campus, Durban 4041, South Africa

report, extracts and fractions of the plant were reported to possess anti-trypanosomal activity [11], but some of the active compounds were not isolated. However, other studies have reported the isolation of niloticane, a cassane diterpene [12], umbelliferone, a coumarin [13], sandynone, niloticane B, and three *seco*-oxacassanes [14] from the plant as well as some flavonoids and phenolic compounds [15]. Docking simulations are based on the optimization of ligand–protein conformations and determine the interactions and mechanism of action of compounds at a binding site [16–18]. Other *Acacia* species have yielded some *seco*-oxacassanes and unusual diterpenoids such as schaffnerine from *Acacia schaffneri* (S.Watson) F.J.Herm. (Syn. of *Vachellia schaffneri* [S.Watson] Seigler & Ebinger) [19,20]. In our continued search for natural compounds that could serve as leads for anti-parasitic drug discovery [21], especially against Human African Trypanosomiasis and African Animal Trypanosomiasis which are neglected tropical diseases still plaguing Africa [1], and chagas disease, a further phytochemical study on the root bark of *V. nilotica* has been carried out in the present study and the isolation and docking study of a novel labdane diterpene is hereby reported. American trypanosomiasis is often referred to as Chagas disease. It is a type of trypanosomiasis that affects Latin Americans. The disease's causal agent *Trypanosoma cruzi* belongs to a separate subgenus of *Trypanosoma*. The parasite is transmitted by kissing bugs and the disease characteristics are different from African trypanosomiasis transmitted by tse–tse fly.

Nevertheless, animals including dogs, cats, pigs, goats, lagomorphs, rodents, primates, or humans are *T. cruzi's* primary reported hosts. Trypanosomiasis has become more prevalent in urban areas due to immigration and a rise in blood transfusions. Chagas disease affects approximately 16–18 million people and puts over 100 million more at risk and is considered the fourth most common endemic illness in America [22].

2 Rationale and design

Drug discovery encompasses all aspects of chemistry and biological evaluations. Drug or lead compounds are presently being synthesized using rational chemistry or isolated from plants and other natural sources. Using ethnobotanical and phytochemical methods, several drugs have been discovered and are in use today. This study also follows the path of phytochemical screening of a well-known and useful medicinal plant to isolate compounds responsible for its ethnobotanical activity and assay it against a prevalent neglected disease in Africa and other parts of the world.

3 Research design

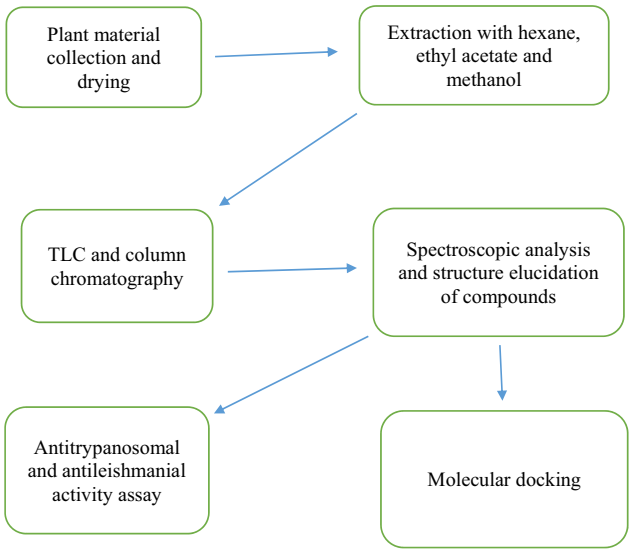

3.1 Materials and methods

3.1.1 General experimental procedure

Column chromatography was carried out using silica gel 60 (0.040–0.063 mm) (230–400 mesh ASTM). Thin-layer chromatography (TLC) was performed on pre-coated aluminium sheets with silica gel F250 (Merck, Germany). Nuclear magnetic resonance (^{1}H, ^{13}C [Dept-q], COSY, HSQC, HMBC, and NOESY) spectra were acquired on a Bruker AVIII (400 MHz) spectrophotometer using $CDCl_3$ as solvent, and spectra were referenced against the residual solvent peak. High-resolution mass spectra were acquired on an Agilent 6130B Single Quadrupole LC/MS System.

3.1.2 Plant material

Roots of *V. nilotica* were collected from trees growing at the Joseph Sarwuan Tarka University Makurdi. The plant was identified by Mr. Titus Yeke of the College of Forestry and Fisheries of the University. A voucher specimen (UAM/FH/0439) was deposited at the herbarium of the college.

3.1.3 Isolation of compounds

The roots were dried under ambient conditions and powdered using a mortar and pestle. The plant powder (500 g) was macerated in 2 L of *n*-hexane for 48 h with intermittent stirring and thereafter filtered to obtain the hexane extract.

Then, 2 L of ethyl acetate were added to the marc and left to stand with stirring for another 48 h and filtered to obtain the ethyl acetate extract. The solvents were removed from the extracts to yield the hexane (1.80 g) and ethyl acetate (2.60 g) extracts. The whole extracts were each subjected to silica gel column chromatography, wet packed in hexane, and eluted with hexane (250 mL) and then 200 mL of gradient amounts (10% increase each time) of ethyl acetate in hexane. The fractions were examined by TLC using a solvent mixture of 3:7 ethyl acetate in hexane. Similar fractions were combined and allowed to dry in a fume hood. The compounds obtained from the hexane extract were stearic acid waxy crystals ([62.8 mg] [fractions 12–14] [compound **4**]), and lupeol ([30.0 mg] [fractions 9–10] [compound **5]**), while

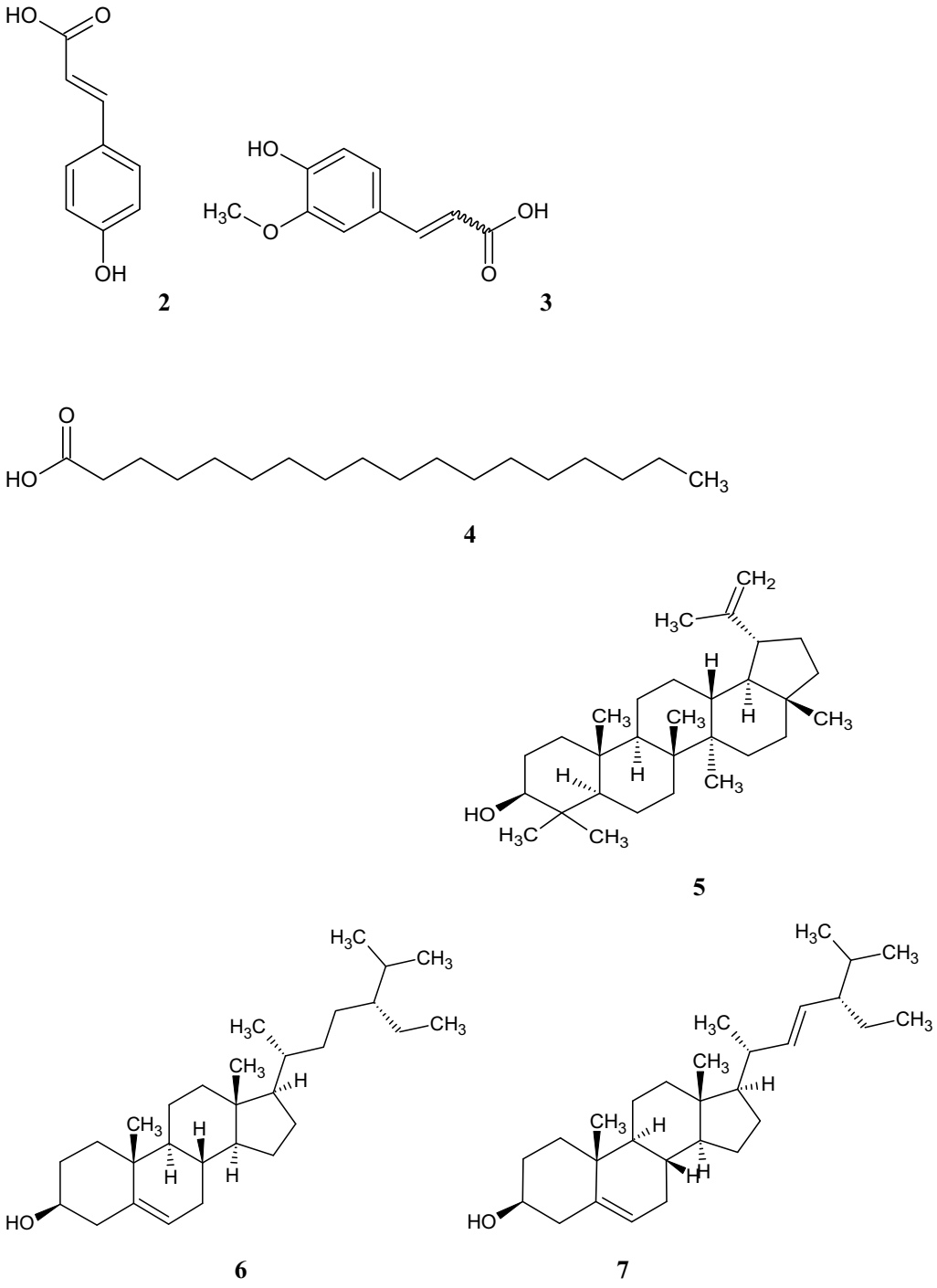

Figure 1: Other compounds isolated.

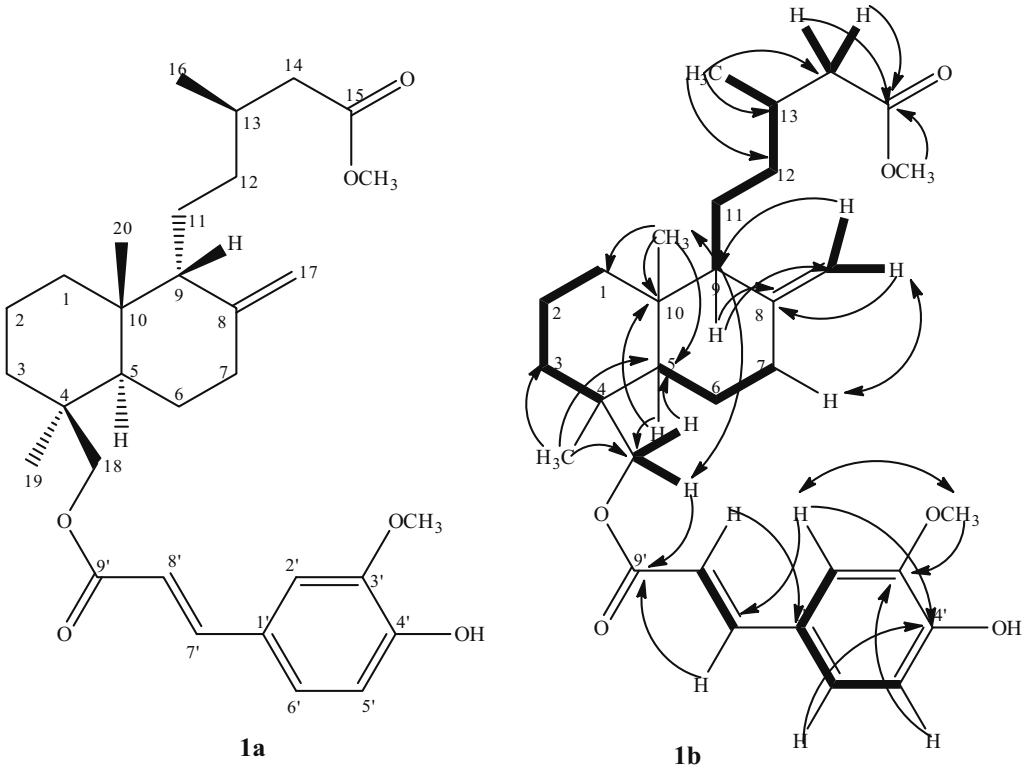

Figure 2: Structure of compound **1** and selected COSY ▬ HMBC ⌒ and NOESY ⇄ correlations.

from the ethyl acetate extract, compound **1** (208.0 mg [fractions 64–70]), compound **2** ([24.0 mg] [fractions 76–77]), compound **3** ([41.0 mg] [fractions 71–75]), and a mixture of compounds **6** and **7** in ratio 1 : 2 ([98.0 mg] [fractions 54–60]) as white crystalline solids were isolated (Figure 1). Their structures were determined or elucidated by NMR spectra (1D and 2D) and where necessary confirmed by HR-ESI.

3.1.4 *In vitro* anti-trypanosomal and anti-leishmanial activity of compound 1

Compound **1** was tested against BSF *T. b. brucei* S427 WT and *L. major* WT promastigotes to assess its anti-parasitic activity using a resazurin-based assay as previously described [23–27]. A stock solution of 20 mg/mL of the compound was prepared in DMSO. In a 96-well plate (Greiner Bio-one GmbH, Germany), the compound was made in 11 double dilutions, starting at 200 µg/mL and decreasing to 0.19 µg/mL in the 1st–11th well, with the 12th well having no drug. The drugs pentamidine and diminazene are most usually used in cattle, sheep, and goat infections since *Trypanosoma brucei* affects animals, and both *Trypanosoma brucei gambiense* and *Trypanosoma brucei rhodesiense* are subspecies that affect humans. Their solutions and respective dilutions were made in parallel to serve as positive controls. The cells were then placed in the proper medium, adjusted to twice the needed density, and introduced into the wells containing drug dilutions. This was followed by incubation for 48 or 72 h, after which 20 µL of 125 µg/mL of phosphate-buffered saline (PBS; Sigma Aldrich, UK) and Resazurin sodium salt was added. The plates were incubated for 24 or 48 h under the same conditions after which the plates were read using a FLUOstar Optima plate reader (BMGLabtech, United States), λ_{exc} = 544 nm, λ_{em} = 590 nm. The outcomes were presented as half maximal effective concentration (EC_{50}) values, which were calculated by non-linear regression using an equation for a sigmoidal dose–response curve with variable slope (GraphPad Prism 5.0).

3.1.5 Docking studies

Compound **1** was subjected to docking studies on cysteine proteases (CPs) which are found in protozoan parasites to which trypanosomes are grouped. Their roles in pathogenesis, which include cell or tissue penetration, hydrolysis of host or parasite proteins, autophagy, and evasion or modulation of the host immune response, are well recognized, hence making them attractive chemotherapeutic and

Table 1: NMR data for compound **1** (400 MHz in $CDCl_3$, δ in ppm, J in Hz)

Position	Experimental			Literature ($CDCl_3$)* [42]	
	^{1}H δ ppm. (mult, J in Hz)	^{13}C (mult)	Selected HMBC	^{1}H δ ppm (mult, J in Hz)	^{13}C (mult)
1	1.84–1.86 (m), 1.10–1.12 (m)	38.7 (CH_2)		1.09, m, 1.83, m	39.8
2	1.53–1.55 (m)	19.2 (CH_2)		1.59, m, 1.70, m	19.7
3	1.81–1.83 (m), 1.12–1.14 (m)	36.5 (CH_2)		1.47, m	37.2
4	—	37.8 (C)		—	38.3
5	1.30–1.33 (m)	56.5 (CH)		1.51, m	50.8
6	1.42–1.44 (m)	24.7 (CH_2)		1.40, m, 1.69, m	25.6
7	2.42–2.44(m), 1.96–1.98 (m)	39.0 (CH_2)		1.99, m, 2.38, m	39.2
8	—	148.1 (C)		—	149.6
9	1.60–1.62 (m)	57.1 (CH)		1.65, m	58.4
10	—	39.7 (C)		—	40.6
11	1.28 1.30(m)	22.8 (CH_2)		1.42, m, 1.52, m	22.0
12	1.82–1.84 (m), 1.08–1.10 (m)	35.9 (CH_2)		1.16, m, 1.37, m	36.9
13	1.93–1.95 (m)	31.0 (CH)		1.89, m	32.1
14	2.13 (dd, 14.7, 8.0), 2.29 (dd, 14.7, 6.1)	42.1 (CH_2)	C-15, C-16, C-13, C-12	2.08, dd (7.7; 14.6), 2.24, dd (6.6, 14.6)	43.3
15	—	174.0 (C)		—	177.6
16	0.94 (d, 6.6)	19.7 (CH_3)		0.96, d (6.6)	20.0
17	4.82 (d, 1.7), 4.50 (s)	106.9 (CH_2)	C-7, C-9	4.53, s, 4.83, s	107.2
18	4.37 (d, 11.0), 3.98 (d, 11.1)	66.9 (CH_2)	C-3, C-19, C-9′	3.75, d (10.8), 3.99, d (10.8)	73.7
19	0.88 (s)	27.9 (CH_3)		0.89, s	18.0
20	0.72 (s)	15.4 (CH_3)		0.77, s	15.4
1′	—	127.2 (C)	—	—	127.7
2′	7.03 (d, 2.0)	115.9 (CH)	C-4, C-6, C-7	7.06, d (2.0)	115.2
3′	—	146.9 (C)	—	—	147.0
4′	—	148.1 (C)	—	—	149.5
5′	6.91 (d, 8.2)	114.8 (CH)	C-1, C-3	6.78, d (8.2)	116.5
6′	7.07 (dd, 8.2, 2.0)	123.2 (CH)	C-2, C-4, C-7	6.97, dd (2.0, 8.2)	123.0
7′	7.58 (d, 15.9)	144.7 (CH)	C-2, C-6, C-9	7.55, d (15.9)	146.9
8′	6.27 (d, 15.9)	115.9 (CH)	C-1, C-9	6.29, d (15.9)	115.0
9′	—	167.7 (C)	—	—	169.3
3′-OCH_3	3.94 (s)	56.1 (CH_3)	C-3′	—	
15-OCH_3	3.66 (s)	51.5 (CH_3)	C-15		

*^{1}H (400 MHz), ^{13}C (100 MHz), and HMBC data for compound **1** in $CDCl_3$ compared to literature report for *ent*-18-*E*-caffeoyloxy-8(17)-labden-15-oic acid in CD_3OD [42] (clerodane and labdane diterpenoids from *N. sphaerocephala*) (the potential of anti-malarial compounds derived from African medicinal plants. Part I: A pharmacological evaluation of alkaloids and terpenoids).

vaccine targets [28]. The docking was to ascertain the binding capacity of the compound against *Leishmania major* and CP *T. b. rhodesiense*. The crystal structure with proteins was retrieved from a protein data bank (PDB) with codes: 2P7U and 4G5D [29,30] (vinyl sulphones as anti-parasitic agents and a structural basis for drug design) (structures of prostaglandin F synthase from the protozoa *Leishmania major* and *T. cruzi* with NADP). To create the size of the grid box, AutoDock tools 1.5.4 [8] was applied, and the compound was optimized to obtain a minimum structure using Gaussian 09 [31]. The dimensions of X = 22, Y = 24, Z = 26 with 1.00 Å as the grid spacing were used. The Lamarckian genetic algorithm technique was used to obtain an optimum binding site for the ligand (binding of chrysoidine to catalase: spectroscopy, isothermal titration calorimetry, and molecular docking studies) [32]. The Gasteiger charges were computed using the AutoDock-Tools graphical user interface built in MGL Tools [8] (AutoDock4 and AutoDockTools4: automated docking with selective receptor flexibility). The compound in the ground state was optimized using density functional theory (DFT). B3LYP functional [33,34] with 6-31+G(d,p) basis set, which is appropriate for a few heteroatoms [35–37]. The highest occupied molecular orbital (HOMO) and the lowest unoccupied molecular orbital (LUMO) calculations were carried out to determine the reactivity character [38–40].

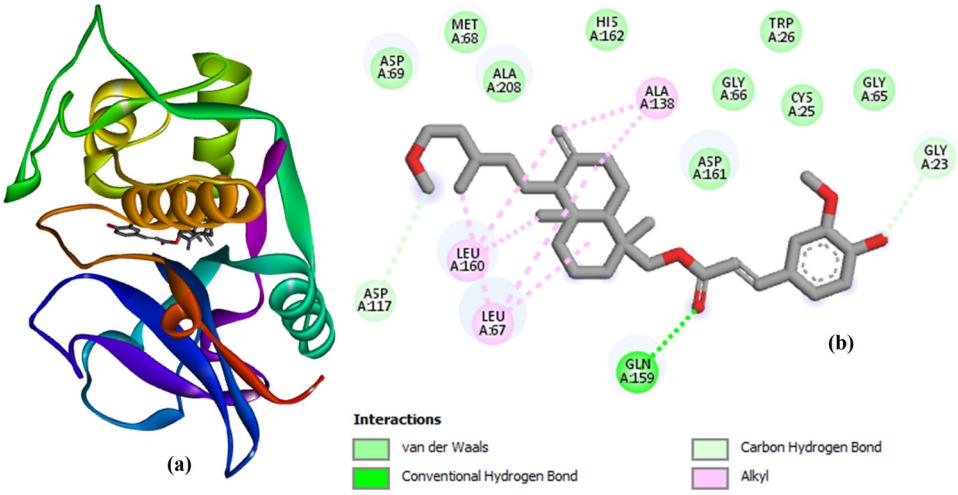

Figure 3: 3D structure of (a) compound **2** in complex CP *Trypanosoma brucei rhodesiense* (b) representations, showing the hydrogen bonding interactions with amino acid residues around the binding pocket.

4 Results and discussion

4.1 Structure elucidation

Compound **1** (Figure 2) was obtained as a white crystalline solid. The molecular formula ($C_{31}H_{44}O_6$) was established based on its sodium adduct ion mass observed under high-resolution ESI at m/z = 535.3035 $[M + Na]^+$ (calc 535.3030) corresponding to $[C_{31}H_{44}NaO_6]^+$. The ^1H NMR (400 MHz, $CDCl_3$) showed two trans-coupled doublets characteristic of the olefinic protons of a cinnamic acid type compound at δ_H (J in Hz) 6.27 (1H, d, J = 15.9, H-8′) and 7.58 ppm (1H, d, J = 15.9, H-7′). The phenyl ring showed three ABX coupled protons at 7.07 (1H, dd, J = 8.2, 2.0, H-6′), 7.03 (1H, d, J = 2.0, H-2′), and 6.91 (1H, d, J = 8.2, H-5′). It also showed one aromatic ring methoxy group at 3.94 (3H, s, 3′-OCH_3) and an ester methoxy at 3.66 (3H, s, 15-OCH_3). The compound showed an aliphatic diterpene component with two ethylenic protons of an exocyclic double bond at 4.50 (1H, d, J = 1.7, H-17a) and 4.82 (1H, d, J = 1.7, H-17b), two methyl singlets at 0.72 (3H, s, H-20) and 1.03 (3H, s, H-19), a methyl doublet at 0.94 (3H, d, J = 6.6, H-16), and three

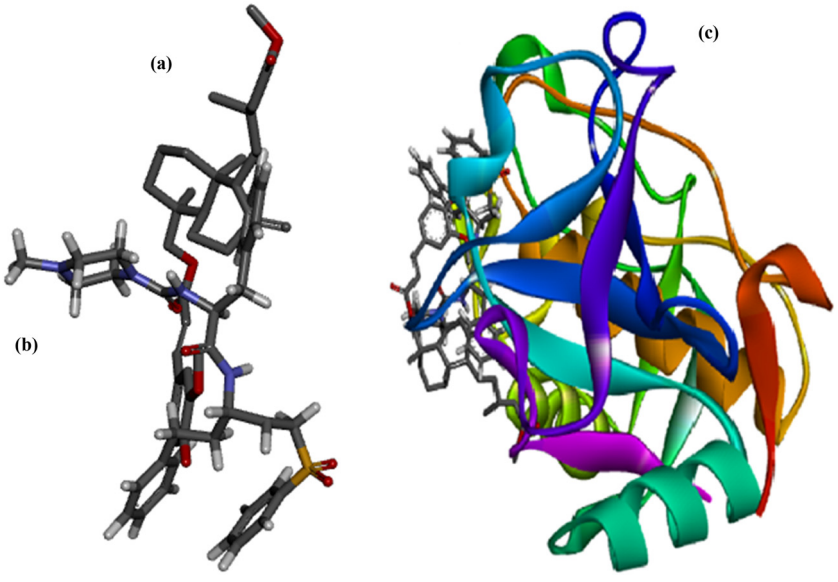

Figure 4: 2D structure (a) of compound **1** aligned with (b) internal ligand (c) 3D representations showing the binding of the isolated compound and the internal ligand in the active binding pocket of CP *Trypanosoma brucei rhodesiense*.

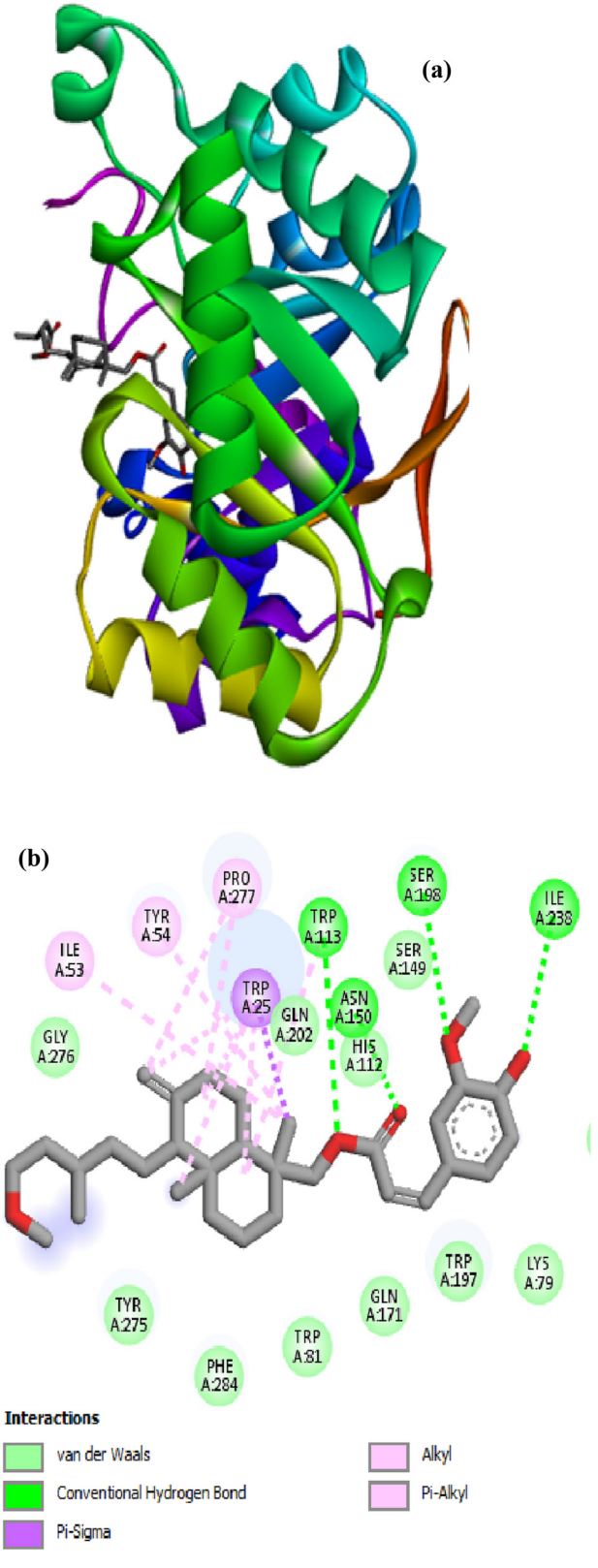

Figure 5: 3D structure (a) of compound **1** in complex *Leishmania major* (b) representations, showing the hydrogen bonding interactions with amino acid residues around the binding pocket.

methines at 1.31 (1H, m, H-5), 1.61 (3H, m, H-9), and 1.93 (1H, m, H-13). Two oxymethylene protons were also observed at 4.37 (1H, d, J = 11.4, H-18a) and 3.98 (1H, d, J = 11.4, H-18b), while the rest of the methylene protons were observed between 1.12 and 2.50 ppm. The ^{13}C NMR (Dept-q) spectrum showed 31 signals including two carbonyl carbons at δ_C 173.9 and 167.7 ppm for two ester carbonyl groups (C-9′ and C-15); two olefinic CH at 116.8 and 144.4; three aromatic CH at 112.9, 119.9, and 125.2; two oxygenated aromatic carbons at 143.3 and 153.0; a quaternary carbon at 126.7; and a methoxy carbon at 56.2 ppm. This part of the structure was identified as a ferulic acid moiety, and its NMR spectral data agreed with literature reports for a feruloyl ester moiety [41] as the carboxylic acid carbon was not that of acid but an ester observed at δ_C 167.7 ppm; hence, it must be esterified. The second part of the spectrum was typical of a diterpene of the 8, (17)-labdene type, and it was represented by 21 carbon signals, including the ester carbonyl at 173.9; an olefinic CH_2 at 106.7 (C-17); a quaternary olefinic carbon at 148.1 (C-8); three methyl carbons at 15.5 (C-20), 19.8 (C-16), 28.1 (C-19); an ester methoxy at 51.8 (C-15–COOCH_3); and an ester oxymethylene (C-18–COOCH_2–) at 67.0 ppm. The rest of the carbons comprised two quaternary carbons at 37.6 (C-4) and 39.6 (C-10); three methines at 56.5 (C-5), 57.1 (C-9), and 30.9 (C-13); and eight methylene carbons between 19.0 and 50.0 ppm. The structure was confirmed by examining the HSQC, COSY, and NOESY correlations and the long-range (^2J and ^3J) correlations in its HMBC spectrum. The COSY spectrum identified all the germinal and vicinal protons, especially the methyl doublet at 0.97 ppm (H-16), the trans-coupled olefinic protons, and the aromatic protons of the ABX spin system. In the HMBC spectrum, a long-range correlation from H-18 to the C-9′ carbonyl confirmed the ester linkage of the ferulic acid to the labdane moiety at C-18, while the correlation from C-15-OCH$_3$ to C-15 also confirmed the methyl ester at C-15. The trans olefinic protons (H-7′ and H-8′) identified C-9′, C-1′, C-2′, and C-6′ while the olefinic protons, H-17 identified C-7 and C-9. The phenolic methoxy confirmed its attachment via a ^3J correlation with C-3′. The rest of the correlations (**1b**) were typical of a labdene diterpene, and the compound was identified as 18α-*O-trans-p*-feruloyl-8(17)-labden-15-methanoate (**1a**). Its relative stereochemistry was determined using correlations in its NOESY spectrum (**1b**) and its chemical shifts (Table 1) compared favourably with a similar *ent*-18-(*E*)-caffeoyloxy-8(17)-labden-15-oic acid isolated from *Nuxia sphaerocephala* (clerodane and labdane diterpenoids from *N. sphaerocephala*) [42]. The compound is not an artefact as the labdane diterpene moiety has not been previously isolated from the plant, and methanol was not used at any point of the isolation and characterization of assay process and procedures; hence, the

Table 2: Anti-parasitic activity of compound **1**

S/No.	Parasite species	Test compound	EC_{50}	pIC50
1	*Trypanosoma brucei*	Compound **1**	9.085 ± 0.966 µg/mL	4.8
		Diminazene	0.0012 ± 0.002 µM/mL	8.7
2	*Leishmania major*	Compound **1**	7.916 ± 0.390 µg/mL	4.8
		Pentamidine	0.638 ± 0.179 µM/mL	6.8

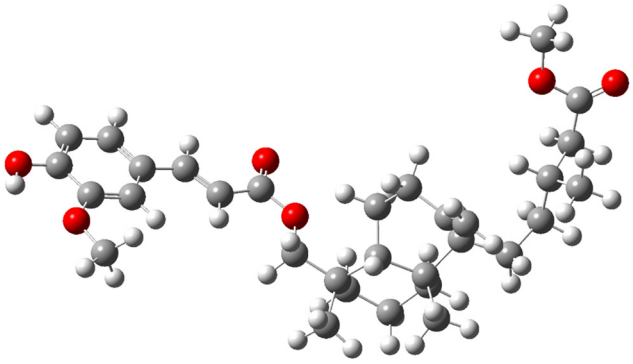

Figure 6: Optimized 2D structure of compound **1** obtained at B3LYP/6-31+G(d,p).

possibility of methylation by methanol does not exist. Other compounds isolated were the phenolic acids; *p*-coumaric acid **2** (phenolic extractives from the root bark of *Picea abies*) [41], ferulic acid **3** (metabolism of ferulic acid by *Paecilomyces variotii* and *Pestalotia palmarum*) [41], the fatty acid stearic acid **4** (determination of the fatty acid profile by ^{1}H NMR spectroscopy) [43], and the triterpenes, lupeol **5** [44] (assignment of ^{1}H and ^{13}C spectra and investigation of hindered side-chain rotation in lupeol derivatives), and a mixture of sitosterol and stigmasterol **6** and **7** (isolation of stigmasterol and sitosterol from the dichloromethane extract of *Rubus suavissimus*) [45]. Their identities were determined and confirmed by comparison to the literature reports and data cited against the compounds. The ^{1}H NMR, ^{13}C NMR, and other spectra for compound **1** are presented in supplementary information (Figures S1–S7).

4.2 Docking analysis

Docking simulation was performed for compound **1** using AutoDocTools. The protein–inhibitor complex containing the isolated compound and the individual interactions with

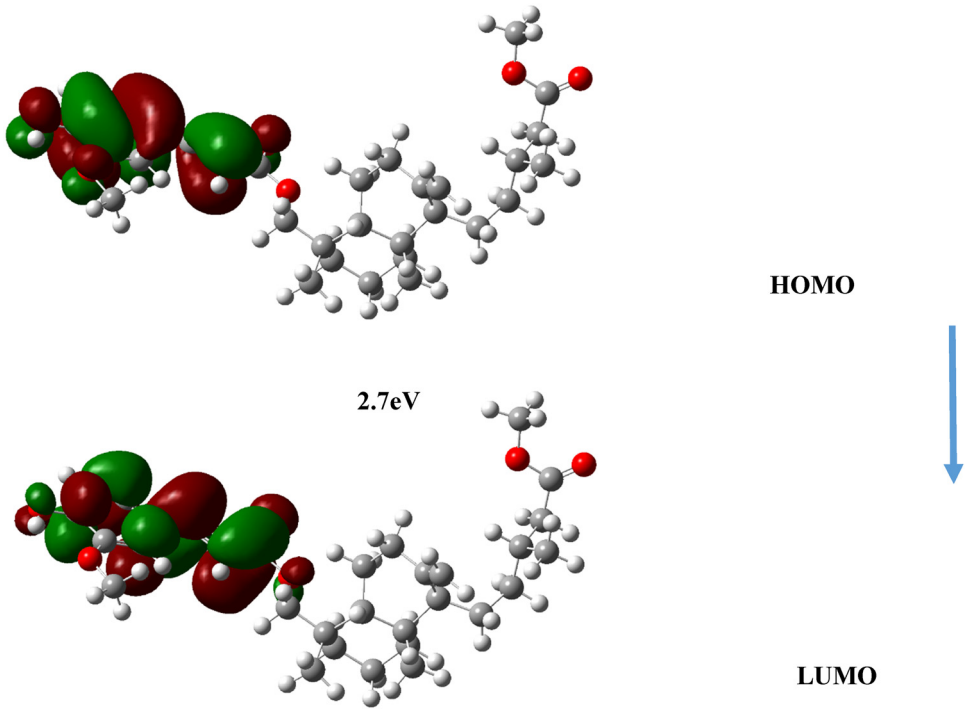

Figure 7: The distribution of electrons of the HOMO is conspicuous around the phenyl ring with high donating ability.

the active site amino acids are presented in Figures 3 and 4. The docking results showed that the isolated compound interacted with the amino acids in the active site of CP *T. b. rhodesiense and Leishmania major*, with a binding energy of −7.8 and −10.5 kcal/mol, respectively. The isolated compound displayed the formation of hydrogen bonding, Pi alkyl, carbon–hydrogen bond, and Van der Waals interactions. As shown in Figures 3 and 4, the carbonyl group of the isolated compound formed hydrogen bonds with glutamine (GLN) 159 of the protease. Notably Van der Waals interaction has been formed with CYS 25, which is the core amino acid residue in the active site of CP *T. b. rhodesiense*. The compound also showed hydrogen bond interactions with SER198, one of the active site amino acid residues of *Leishmania major*. From Figure 4, the compound binds with a higher affinity with *L. major* compared to its binding with *T. b. rhodesiense*. These differences in the binding potentials may be due to the structural conformation of the proteins. The docking protocol was validated by docking the internal ligand with the prepared protein, and the docking is presented in Figures 4 and 5. The docking results show the alignment between the internal ligand and the isolated compound in the active site of CP *T. b. rhodesiense and L. major*. Docking simulations generate binding scores that show the affinity between drugs and targets, while *in vitro* studies investigate the biological responses [18]. The binding energies obtained in this study are similar and agree with the *in vitro* data obtained.

4.3 Anti-trypanosomal and anti-leishmanial activity of compound 1

The pIC_{50} of the compound shows an identical value of 4.8 against *T. brucei* and *L. major* (Table 2). The *in silico* and *in vitro* data, put together, suggest that the compound is promising but needs to be optimized. The binding of the compound with active site amino acid residues of selected proteins could provide insight into proposing the enzyme's catalytic mechanism.

4.4 DFT analysis

The optimized geometries of compound **1** using the DF method are shown in Figure 6.

HOMO–LUMO are described as frontier molecular orbitals [38,46]. The electron-donating ability of a compound is aligned with the $E_{HOMO,}$ and the higher the energy for $E_{HOMO,}$ the higher the ability of the compound to donate electrons [40,47]. The distribution of electrons of the HOMO (Figure 7) is conspicuous around the phenyl ring with high donating ability.

8(17)-Labden-15-oic acid has not been previously isolated or reported from the plant species, and its isolation as a ferulic acid ester is novel. The unesterified ferulic acid isolated confirms its presence as a metabolite, and its esterification to the labdane alcohol is part of compound **1** biosynthetic pathway. It is certainly not a product of esterification during the work up or isolation process of compound **1** as no acids or alkali was used or any esterifying conditions. The other compounds **2–7** were not tested for anti-parasitic activity as they are quite familiar compounds and have been tested previously [48]. The crude extracts and fractions were not tested as they will contain several mixtures and the identity of any active constituent cannot be determined easily.

5 Conclusion

In this study, further phytochemical and biological studies on the root bark of *A. nilotica* have led to the isolation of a novel labdane triterpene, 18α-*O*-*trans*-*p*-feruloyl-8(17)-labden-15-methanoate. The compound demonstrated promising anti-parasitic activity against *T. brucei* and *L. major*. The DFT studies of the compound revealed low Δ*E*, a strong indication of high reactivity. The *silico* study and DFT revealed critical energies that could provide information regarding the catalytic mechanism. Optimized synthetic iterations of the compound could provide essential leads in developing effective drugs against the parasites.

The structure of the novel labdane has been uploaded to PubChem with a release date set for 11 February, 2023, when it can be accessed by the following link: https://pubchem.ncbi.nlm.nih.gov/upload/#substance-118572.

Acknowledgements: The authors acknowledge Kuwait University for allowing using their facilities and space as well as CHPC (www.chpc.ac.za) and UKZN for operational and infrastructural support.

Funding information: Authors state no funding involved.

Author contributions: NFA, JVA, JOI, AIG and EYS carried out the isolation, purification, structure elucidation and bioassay of the compound and wrote the first draft. CUI performed the *in silico* studies and wrote the second draft. NFA and JOI supervised, edited, and revised the manuscript. All authors analysed, read, edited, and approved

the final manuscript. Naser F. Al-Tannak and John V. Anyam are joint first authors.

Conflict of interest: Authors declare no conflict of interest.

Ethical approval: The conducted research is not related to either human or animal use.

Data availability statement: All data generated or analysed during this study are included in this published article (and its supplementary information files).

References

[1] Igoli JO, Teles YC, Atawodi SE, Ferro VA, Watson DG. Ethnopharmacological strategies for drug discovery against African neglected diseases. Front Pharmacol. 2022;13:851064. doi: 10.3389/fphar.2022.851064.

[2] Ribeiro-Filho J, Teles YC, Igoli JO, Capasso R. New trends in natural product research for inflammatory and infectious diseases. Front Pharmacol. 2023;14:1144074. doi: 10.3389/fphar.2023.1144074.

[3] Rao SA, Shetty NP. Structure-based screening of natural product libraries in search of potential antiviral drug-leads as first-line treatment to COVID-19 infection. Microb Pathog. 2022;165:105497. doi: 10.1016/j.micpath.2022.105497.

[4] Wilson BA, Thornburg CC, Henrich CJ, Grkovic T, O'Keefe BR. Creating and screening natural product libraries. Nat Prod Rep. 2020;37:893–918. doi: 10.1039/C9NP00068B.

[5] Onguéné PA, Simoben CV, Fotso GW, Andrae-Marobela K, Khalid SA, Ngadjui BT, et al. In silico toxicity profiling of natural product compound libraries from African flora with anti-malarial and anti-HIV properties. Comput Biol Chem. 2018;72:136–49. doi: 10.1016/j.compbiolchem.2017.12.002.

[6] Roncaglioni A, Toropovv AA, Toropova AP, Benfenati E. In silico methods to predict drug toxicity. Curr Opin Pharmacol. 2013;5:802–6. doi: 10.1016/j.coph.2013.06.001.

[7] Choudhary S, Tak N, Bissa G, Chouhan B, Choudhary P, Sprent JI, et al. The widely distributed legume tree *Vachellia* (*Acacia*) *nilotica* subsp. indica is nodulated by genetically diverse Ensifer strains in India. Symbiosis. 2020;80:15–31. doi: 10.1007/s13199-019-00658-8.

[8] Morris GM, Huey R, Lindstrom W, Sanner MF, Belew RK, Goodsell DS, et al. AutoDock4 and AutoDockTools4: Automated docking with selective receptor flexibility. J Comput Chem. 2009;30(16):2785–91. doi: 10.1002/jcc.21256.

[9] Elbanna SM. Ant–Acacia interaction: Chemical or physical defense? Entomol Res. 2011;41(4):135–41. doi: 10.1111/j.1748-5967.2011.00330.x.

[10] Qasim M, Abideen Z, Adnan MY, Ansari R, Gul B, Khan M. Traditional ethnobotanical uses of medicinal plants from coastal areas. J coast life Med. 2014;2(1):22–30. doi: 10.12980/JCLM.2.2014C1177.

[11] Ogbadoyi E, Garba M, Kabiru A, Mann A, Okogun J. Original Report Therapeutic evaluation of *Acacia nilotica* (Linn) stem bark extract in experimental African trypanosomiasis. Int J Appl Res Nat Prod. 2011;4(2):11–8.

[12] Eldeen I, Van Heerden F, Van Staden J. In vitro biological activities of niloticane, a new bioactive cassane diterpene from the bark of *Acacia nilotica* subsp. kraussiana. J Ethnopharmacology. 2010;128(3):555–60. doi: 10.1016/j.jep.2010.01.057.

[13] Singh R, Singh B, Singh S, Kumar N, Kumar S, Arora S. Umbelliferone–An antioxidant isolated from *Acacia nilotica* (L.) Willd. ex. Del. Food Chem. 2010;120(3):825–30. doi: 10.1016/j.foodchem.2009.11.022.

[14] Anyam JV, Daikwo PE, Ungogo MA, Nweze NE, Igoli NP, Gray AI, et al. Two new antiprotozoal diterpenes from the roots of *Acacia nilotica*. Front Chem. 2021;9:624741. doi: 10.3389/fchem.2021.624741.

[15] Saleem N. An ethno-pharmacological study of Egyptian Bedouin women's knowledge of medicinal plants; 2012. https://stax.strath.ac.uk/concern/theses/nk322d36m. Accessed 24 Sep 2023.

[16] Meng XY, Zhang HX, Mezei M, Cui M. Molecular docking: a powerful approach for structure-based drug discovery. Curr Comput drug Des. 2011;7(2):146–57.

[17] Pinzi L, Rastelli G. Molecular docking: shifting paradigms in drug discovery. Int J Mol Sci. 2019;20(18):4331. doi: 10.3390/ijms20184331.

[18] Cava C, Castiglioni I. Integration of molecular docking and in vitro studies: a powerful approach for drug discovery in breast cancer. Appl Sci. 2020;10(19):6981. doi: 10.3390/app10196981.

[19] Manríquez-Torres JJ, Torres-Valencia JM, Velázquez-Jiménez R, Valdez-Calderón A, Alvarado-Rodriguez JG, Cerda-Garcia-Rojas CM, et al. A macrocyclic dimeric diterpene with a C2 symmetry axis. Org Lett. 2013;15(18):4658–61. doi: 10.1021/ol401890v.

[20] Manríquez-Torres JJ, Torres-Valencia JM, Gómez-Hurtado MA, Motilva V, García-Mauriño S, Ávila J, et al. Absolute configuration of 7,8-seco-7,8-oxacassane diterpenoids from *Acacia schaffneri*. J Nat Prod. 2011;74(9):1946–195. doi: 10.1021/np200445y.

[21] Ungogo MA, Ebiloma GU, Ichoron N, Igoli JO, De Koning HP, Balogun EO. A review of the antimalarial, antitrypanosomal, and antileishmanial activities of natural compounds isolated from Nigerian flora. Front Chem. 2020;8:617448. doi: 10.3389/fchem.2020.617448.

[22] Rosypal AC, Cortés-Vecino JA, Gennari SM, Dubey JP, Tidwell RR, Lindsay DS. Serological survey of *Leishmania infantum* and *Trypanosoma cruzi* in dogs from urban areas of Brazil and Colombia. Vet Parasitol. 2007;149(3-4):172–7.

[23] Gould MK, Vu XL, Seebeck T, De Koning HP. Propidium iodide-based methods for monitoring drug action in the kinetoplastidae: Comparison with the Alamar Blue assay. Anal Biochem. 2008;382(2):87–93. doi: 10.1016/j.ab.2008.07.036.

[24] Fueyo Gonzalez FJ, Ebiloma GU, Izquierdo Garcia C, Bruggeman V, Sanchez Villamanan JM, Donachie A, et al. Conjugates of 2,4-dihydroxybenzoate and salicylhydroxamate and lipocations display potent antiparasite effects by efficiently targeting the Trypanosoma brucei and Trypanosoma congolense mitochondrion. J Med Chem. 2017;60(4):1509–22. doi: 10.1021/acs.jmedchem.6b01740.

[25] Eze FI, Noundou XS, Osadebe PO, Krause RW. Phytochemical, anti-inflammatory and anti-trypanosomal properties of *Anthocleista vogelii* Planch (Loganiaceae) stem bark. J Ethnopharmacol. 2019;238:111851. doi: 10.1016/j.jep.2019.111851.

[26] Khandazhinskaya AL, Matyugina ES, Solyev PN, Wilkinson M, Buckheit KW, Buckheit Jr RW, et al. Investigation of 5'-norcarbocyclic nucleoside analogues as antiprotozoal and antibacterial

agents. Molecules. 2019;24(19):3433. doi: 10.3390/molecules24193433.
[27] Nvau JB, Alenezi S, Ungogo MA, Alfayez IA, Natto MJ, Gray AI, et al. Antiparasitic and cytotoxic activity of bokkosin, a novel diterpene-substituted chromanyl benzoquinone from *Calliandra portoricensis*. Front Chem. 2020;8:574103. doi: 10.3389/fchem.2020.574103.
[28] Siqueira-Neto JL, Debnath A, McCall LI, Bernatchez JA, Ndao M, Reed SL, et al. Cysteine proteases in protozoan parasites. PLoS Neglected Trop Dis. 2018;23(12(8)):e0006512. doi: 10.1371/journal.pntd.0006512<PMID: 30138453; PMCID: PMC6107107.
[29] Kerr ID, Lee JH, Farady CJ, Marion R, Rickert M, Sajid M, et al. Vinyl sulfones as antiparasitic agents and a structural basis for drug design. J Biol Chem. 2009;284(38):25697–703. doi: 10.1074/jbc.M109.014340.
[30] Moen SO, Fairman JW, Barnes SR, Sullivan A, Nakazawa-Hewitt S, Van Voorhis WC, et al. Structures of prostaglandin F synthase from the protozoa *Leishmania major* and *Trypanosoma cruzi* with NADP. Acta Crystallogr Sect F Struct Biol Commun. 2015;F71:609–14. doi: 10.1107/S2053230X15006883.
[31] Frisch M, Trucks G, Schlegel H, Scuseria G, Robb M, Cheeseman J, et al. 09, Revision D. 01. Wallingford, CT: Gaussian, Inc; 2009.
[32] Yang B, Hao F, Li J, Chen D, Liu R. Binding of chrysoidine to catalase: spectroscopy, isothermal titration calorimetry and molecular docking studies. J Photochem Photobiol B. 2013;128:35–42. doi: 10.1016/j.jphotobiol.2013.08.006.
[33] Kohn W, Becke AD, Parr RG. Density functional theory of electronic structure. J Phys Chem. 1996;100(31):12974–80. doi: 10.1021/jp960669l.
[34] Becke AD. Density-functional thermochemistry. I. The effect of the exchange-only gradient correction. J Chem Phys. 1993;96:2155–60. doi: 10.1063/1.462066.
[35] Ekennia AC, Osowole AA, Olasunkanmi LO, Onwudiwe DC, Olubiyi OO, Ebenso EE. Synthesis, characterization, DFT calculations and molecular docking studies of metal (II) complexes. J Mol Struct. 2017;1150:279–92. doi: 10.1016/j.molstruc.2017.08.085.
[36] Gorelsky SI, Basumallick L, Vura-Weis J, Sarangi R, Hodgson KO, Hedman B, et al. Spectroscopic and DFT Investigation of [M {HB (3, 5-i Pr2pz) 3}(SC6F5)](M = Mn, Fe, Co, Ni, Cu, and Zn) Model Complexes: Periodic Trends in Metal− Thiolate Bonding. Inorg Chem. 2005;44(14):4947–60. doi: 10.1021/ic050371m.
[37] Chioma F, Ekennia AC, Ibeji CU, Okafor SN, Onwudiwe DC, Osowole AA, et al. Synthesis, characterization, antimicrobial activity and DFT studies of 2-(pyrimidin-2-ylamino) naphthalene-1, 4-dione and its Mn (II), Co (II), Ni (II) and Zn (II) complexes. J Mol Struct. 2018;1163:455–64. doi: 10.1016/j.molstruc.2018.03.025.
[38] Rauf SM, Arvidsson PI, Albericio F, Govender T, Maguire GE, Kruger HG, et al. The effect of N-methylation of amino acids (Ac-X-OMe) on solubility and conformation: a DFT study. Org Biomol Chem. 2015;13:9993–10006. doi: 10.1039/C5OB01565K.
[39] Fakhar Z, Govender T, Lamichhane G, Maguire GE, Kruger HG, Honarparvar B. Computational model for the acylation step of the β-lactam ring: Potential application for l,d-transpeptidase 2 in mycobacterium tuberculosis. J Mol Struct. 2017;1128:94–102. doi: 10.1016/j.molstruc.2016.08.049.
[40] Ibeji CU, Adejoro IA, Adeleke BB. A benchmark study on the properties of unsubstituted and some substituted polypyrroles. J Phys Chem & Biophysics. 2015;5(6):193.
[41] Rahouti M, Seigle-Murandi F, Steiman R, Eriksson K. Metabolism of ferulic acid by Paecilomyces variotii and Pestalotia palmarum. Appl Environ Microbiol. 1989;55(9):2391–8. doi: 10.1128/aem.55.9.2391-2398.1989.
[42] Mambu L, Grellier P, Florent L, Joyeau R, Ramanitrahasimbola D, Rasoanaivo P, et al. Clerodane and labdane diterpenoids from *Nuxia sphaerocephala*. Phytochemistry. 2006;67(5):444–51. doi: 10.1016/j.phytochem.2005.11.024.
[43] Knothe G, Kenar JA. Determination of the fatty acid profile by ^{1}H-NMR spectroscopy. Eur J Lipid Sci Technol. 2004;106(2):88–96. doi: 10.1002/ejlt.200300880.
[44] Burns D, Reynolds WF, Buchanan G, Reese PB, Enriquez RG. Assignment of 1H and 13C spectra and investigation of hindered side-chain rotation in lupeol derivatives. Magn Reson Chem. 2000;38(7):488–93. doi: 10.1002/1097-458X(200007)38:7<488:AID-MRC704>3.0.CO;2-G.
[45] Chaturvedula VS, Prakash I. Isolation of Stigmasterol and β-Sitosterol from the dichloromethane extract of Rubus suavissimus. Int Curr Pharm J. 2012;1(9):239–42.
[46] Dumont RS. Effects of charging and polarization on molecular conduction via the source-sink potential method. Can J Chem. 2013;92(2):100–11. doi: 10.1139/cjc-2013-0227.
[47] Ekennia AC, Osowole AA, Onwudiwe DC, Babahan I, Ibeji CU, Okafor SN, et al. Synthesis, characterization, molecular docking, biologicalactivity and density functional theory studies of novel 1,4-naphthoquinone derivatives and Pd(II), Ni(II) and Co(II) complexes. Appl Organomet Chem. 2018;32(5):e4310. doi: 10.1002/aoc.4310.
[48] Ebiloma GU, Ichoron N, Siheri W, Watson DG, Igoli JO, De Koning HP. The strong anti-kinetoplastid properties of bee propolis: Composition and identification of the active agents and their biochemical targets. Molecules. 2020;25(21):5155. doi: 10.3390/molecules25215155.